Three-level direct torque control based on space vector modulation of double star synchronous machine

Elakhdar Benyoussef, Abdelkader Meroufel, and Said Barkat

***Abstract*—** This paper presents a direct torque control based on space vector modulation of the salient-pole double star synchronous machine drive fed by two three-level neutral point clamped inverters. This type of inverters has several advantages over the standard two-level inverter, such as a greater number of levels in the output voltage waveforms, less harmonic distortion in voltage and current waveforms and lower switching frequencies. The conventional direct torque control drives utilizing hysteresis comparators suffer from high torque ripple and variable switching frequency. The most common solution to those problems is to use the space vector depends on the reference torque and flux. Simulations results are included to verify the effectiveness of the proposed control method under load disturbances and speed reference variations.

***Keywords*—** Double Star Synchronous Machine, Multi-Level Inverter, Direct Torque Control, Space Vector Modulation.

I. INTRODUCTION

NOWDAYS, many industry segments need high power electrical drives with the well-known requirements like high efficiency, high power density and reliability [1]. High-power electric drive systems are required in many applications, such as traction, electric/hybrid vehicles, and ship propulsion [2]. The common exigency between the aforementioned applications is the use of high power machine. In this context, multiphase AC machines have been recognized as a viable approach to obtain higher power ratings based on the concept of power segmentation. In multiphase drive, the number of phases of the machine is not restricted to three and it is chosen according the power demand.

Multiphase machine possess several advantages over conventional three phase machine. These include increasing the inverter output power, reducing the amplitude of torque ripple and lowering the DC link current harmonics [3]. Multiphase drive system improves the reliability; the motor can start and run since the loss of one or many phase. For high power, the use of the synchronous machine specially finds its application in the motorization at variable speed of the embedded systems [4]. But when they are supplied by thyristor current source inverter, torque ripples of high amplitude appear. Increasing the number of triple armature windings, which is supplied in relation to each other one, lowers the rate of the torque ripples. Especially, the first harmonic of double star synchronous machine is twelve times the operating frequency of the machine.

In the other hand, multilevel inverter fed electric machine systems are considered as a promising approach in achieving high power/high voltage ratings. Moreover, multilevel inverters have the advantages of overcoming voltage limit capability of semiconductor switches, and improving 2 harmonic profiles of output waveforms [5], [6]. The output voltage waveform approaches a sine wave, thus having practically no common-mode voltage and no voltage surge to the motor windings. Furthermore, the reduction in d*v*/d*t* can prevent motor windings and bearings from failure.

The direct torque control (DTC) has been recognized as the most promising solution to achieve these requirements. The DTC is based on the decoupled control of flux and torque providing a very quick and robust response [7]. Its simplicity, robustness and fast torque response are the major factors make it popular in industries [8]. Common disadvantages of conventional DTC are high torque ripple and slow transient response to the step changes in torque during start-up. Several techniques have been developed to improve the torque performance. One of them is to reduce the ripples is based on space vector modulation (SVM) technique [9].

To improve the performances of a double star synchronous machine, a three-level DTC based on space vector modulation (DTC-SVM) is proposed in this paper.

This paper is organized as follows. Section II presents the model of the DSSM. The proposed three-level neutral point clamped (NPC) inverter controlled via space vector modulation (SVM) is discussed in Sections III. In section IV deals with the conventional direct torque control. The direct torque control based on space vector modulation strategy is described in Section V. In Section VI summarizes and comments the simulation results obtained, while Section VII concludes the paper.

E. Benyoussef is with the Intelligent Control & Electrical Power Systems laboratory, Djillali Liabes University, Sidi Bel Abbes, Algeria. (E-mail: lakhdarbenyoussef@yahoo.com).
A. Meroufel is with the Intelligent Control & Electrical Power Systems laboratory, Djillali Liabes University, Sidi Bel Abbes, Algeria. (E-mail: ameroufel@yahoo.fr).
S. Barkat is with the Faculty of Science and Engineering, Department of Electrical Engineering, M'sila University, Ichbilia Street, M'sila 28000, Algeria. (E-mail: Sa_Barkati@yahoo.fr).

II. Double Star Synchronous Machine Model

The voltage equations of the double star synchronous machine are as follows:

$$v_s = Ri_s + \frac{d}{dt}\phi_s \tag{1}$$

The stator resistance matrix for each star is diagonal 3×3 matrix is given by: $R = Diag\begin{bmatrix} R_s & R_s & R_s \end{bmatrix}$.

The original six dimensional system of the machine can be decomposed into three orthogonal subspaces (α,β), (z_1,z_2) and (z_3,z_4), using the following transformation:

$$\begin{bmatrix} F_\alpha & F_\beta & F_{z1} & F_{z2} & F_{z3} & F_{z4} \end{bmatrix} = \begin{bmatrix} T \end{bmatrix}\begin{bmatrix} F_s \end{bmatrix} \tag{2}$$

With

$$\begin{bmatrix} F_s \end{bmatrix} = \begin{bmatrix} F_{s1} & F_{s2} \end{bmatrix}^T = \begin{bmatrix} F_{a1} & F_{b1} & F_{c1} & F_{a2} & F_{b2} & F_{c2} \end{bmatrix}^T$$

Where: F_s can be used for stator currents (i_s), stator flux (ϕ_s), and stator voltages (v_s).

The matrix T is given by:

$$[T] = \frac{1}{\sqrt{3}}\begin{pmatrix} \cos(0) & \cos\left(\frac{2\pi}{3}\right) & \cos\left(\frac{4\pi}{3}\right) & \cos(\gamma) & \cos\left(\frac{2\pi}{3}+\gamma\right) & \cos\left(\frac{4\pi}{3}+\gamma\right) \\ \sin(0) & \sin\left(\frac{2\pi}{3}\right) & \sin\left(\frac{4\pi}{3}\right) & \sin(\gamma) & \sin\left(\frac{2\pi}{3}+\gamma\right) & \sin\left(\frac{4\pi}{3}+\gamma\right) \\ \cos(0) & \cos\left(\frac{4\pi}{3}\right) & \cos\left(\frac{2\pi}{3}\right) & \cos(\pi-\gamma) & \cos\left(\frac{\pi}{3}-\gamma\right) & \cos\left(\frac{5\pi}{3}-\gamma\right) \\ \sin(0) & \sin\left(\frac{4\pi}{3}\right) & \sin\left(\frac{2\pi}{3}\right) & \sin(\pi-\gamma) & \sin\left(\frac{\pi}{3}-\gamma\right) & \sin\left(\frac{5\pi}{3}-\gamma\right) \\ 1 & 1 & 1 & 0 & 0 & 0 \\ 0 & 0 & 0 & 1 & 1 & 1 \end{pmatrix} \tag{3}$$

The Park model of the DSSM in the rotor reference frame (*d*-*q*) is defined by the following equations system:

$$\begin{cases} v_d = R_s i_d + \dfrac{d\phi_d}{dt} - \omega\phi_q \\ v_q = R_s i_q + \dfrac{d\phi_q}{dt} + \omega\phi_d \end{cases} \tag{4}$$

Where:

$$\begin{cases} \phi_d = L_d i_d + M_{fd} i_f \\ \phi_q = L_q i_q \end{cases} \tag{5}$$

With:
v_d, v_q : Stator voltages *dq* components.
i_d, i_q : Stator currents *dq* components.
ϕ_d, ϕ_q : Stator flux *dq* components.

The rotor voltage equation is given by:

$$v_f = R_f i_f + \frac{d\phi_f}{dt} \tag{6}$$

The mechanical equation is given by:

$$J\frac{d\Omega}{dt} = T_{em} - T_L - f_r\Omega \tag{7}$$

With:
T_{em}, T_L : Electromagnetic and load torque.
Ω : Rotor speed.
v_f, i_f : Voltage and current of rotor excitation.

The electromagnetic torque generated by the machine is:

$$T_{em} = p\left(\phi_d i_q - \phi_q i_d\right) \tag{8}$$

III. Three-Level Inverter Modelling

A three-level inverter differs from a conventional two-level inverter in that it is capable of producing three different levels of output phase voltage. The structure of a three-level neutral point clamped inverter is shown in figure 1. When switches 1 and 2 are on the output is connected to the positive supply rail. When switches 3 and 4 are on, the output is connected to the negative supply rail. When switches 2 and 3 are on, the output is connected to the supply neutral point via one of the two clamping diodes [6].

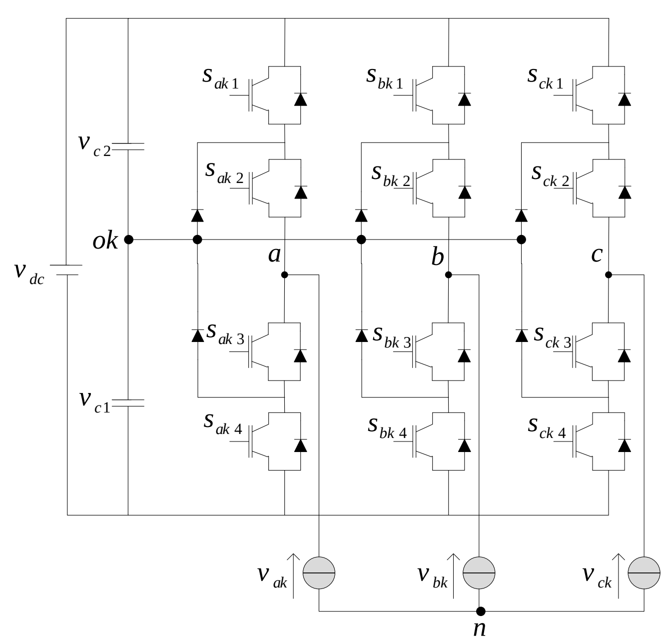

Fig. 1 Three-level inverter (k =1 for first inverter and k =2 for second inverter).

Functions of connection are given by:

$$\begin{cases} F_{xk2} = s_{xk1}.s_{xk2} \\ F_{xk1} = s_{xk3}.s_{xk2} \end{cases}, \quad x = a,b,c \tag{9}$$

The phase voltages v_{ak}, v_{bk}, v_{ck} can be written as:

$$\begin{pmatrix} v_{ak} \\ v_{bk} \\ v_{ck} \end{pmatrix} = \begin{pmatrix} 2F_{ak2} - F_{bk2} - F_{ck2} & 2F_{ak1} - F_{bk1} - F_{ck1} \\ 2F_{bk2} - F_{ak2} - F_{ck2} & 2F_{bk1} - F_{ak1} - F_{ck1} \\ 2F_{ck2} - F_{ak2} - F_{bk2} & 2F_{ck1} - F_{ak1} - F_{bk1} \end{pmatrix} \begin{pmatrix} v_{dc} \\ v_{dc}/2 \end{pmatrix} \tag{10}$$

The representation of the space voltage vectors of a three-level inverter for all switching states is given by figure 2. According to the magnitude of the voltage vectors, the voltage vectors can be partitioned into four groups: the zero voltage vectors (v_0), the large voltage vectors (v_{1L}, v_{3L}, v_{5L}, v_{7L}, v_{9L}, v_{11L}), the middle voltage vectors (v_{2L}, v_{4L}, v_{6L}, v_{8L}, v_{10L}, v_{12L}), and the small voltage vectors (v_{1S}, v_{2S}, v_{3S}, v_{4S}, v_{5S}, v_{6S}).

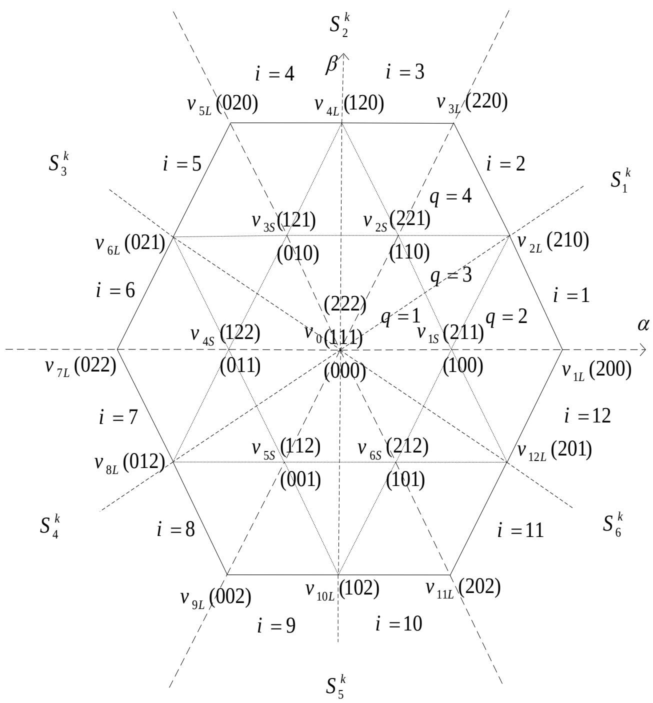

Fig. 2 Space vector diagram showing switching states for a three-level inverter.

The SVM methods provide flexibility to select and optimize switching patterns to (i) minimize harmonics, (ii) modify the switching pattern to carry out DC-capacitor voltages balancing task with no requirement for additional power circuitry, and (iii) minimize switching frequency for high power applications. However, real-time implementation of the conventional SVM strategies is faced with time limits due to the calculation overhead time. Therefore, fast algorithms are required to overcome complexity of calculations. A fast SVM algorithm can save the processor execution time to perform the required calculations of DC-capacitor voltages balancing task.

A. Determination of the sector numbers

The reference vector magnitude and angle are determined from:

$$\begin{cases} u_{refk} = \sqrt{u_{ref\,\alpha k}^2 + u_{ref\,\beta k}^2} \\ \vartheta_k = \tan 2^{-1}\left(\dfrac{u_{ref\,\beta k}}{u_{ref\,\alpha k}}\right) \end{cases} \tag{11}$$

Where the $\tan 2^{-1}$ function returns an angle $-\pi \le \vartheta_k \le \pi$ which is converted into the range $0 \le \vartheta_k \le 2\pi$ by a C subroutine.

The sector numbers *1-6* is given by:

$$S_n^k = ceil\left(\frac{\vartheta_k}{\pi/3}\right) \in \{1,\ 2,\ 3,\ 4,\ 5,\ 6\} \tag{12}$$

Where ceil is the C-function that adjusts any real number to the nearest, but higher, integer [e.g. ceil (3.1) = 4], (*n=1… 6*).

B. Identification of the triangles

The reference vector is projected on the two axes making 60° between them. In each sector S_n^k, components $u_{refk1}^{S_n^k}$ and $u_{refk2}^{S_n^k}$ are given by:

$$\begin{aligned} u_{refk1}^{S_n^k} &= 2M_k\left(\cos(\vartheta_k - (S_n^k - 1)\frac{\pi}{3}) - \frac{1}{\sqrt{3}}\sin(\vartheta_k - (S_n^k - 1)\frac{\pi}{3})\right) \\ u_{refk2}^{S_n^k} &= 2M_k\left(\frac{2}{\sqrt{3}}\sin(\vartheta_k - (S_n^k - 1)\frac{\pi}{3})\right) \end{aligned} \tag{13}$$

The modulation factor M_k is given by:

$$M_k = \frac{u_{refk}}{v_{dc}\sqrt{2/3}} \tag{14}$$

In order to determine the number of the triangle in a sector S_n^k, the two following entireties are to be defined:

$$\begin{aligned} l_{k1}^{S_n^k} &= \mathrm{int}(u_{refk1}^{S_n^k}) \\ l_{k2}^{S_n^k} &= \mathrm{int}(u_{refk2}^{S_n^k}) \end{aligned} \tag{15}$$

Where: *int* is a function which gives the whole part of a given real number.

The figure 3 presents the projection of u_{refk} in the first sector

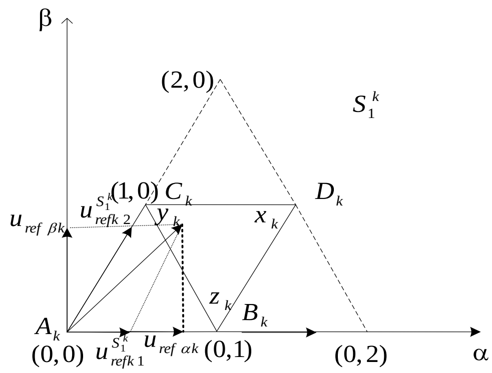

Fig. 3 First sector corresponding to the space voltage vectors of a three-level inverter.

In a reference mark formed by the two vectors $u_{refk\,1}^{S_n^k}$ and $u_{refk\,2}^{S_n^k}$ the coordinates of the tops A_k, B_k, C_k and D_k are given by:

$$\begin{aligned}
\left(u_{A_{k1}}^{\Delta_q^{S_n^k}},\ u_{A_{k2}}^{\Delta_q^{S_n^k}}\right) &= \left(l_{k1}^{S_n^k},\ l_{k2}^{S_n^k}\right)\\
\left(u_{B_{k1}}^{\Delta_q^{S_n^k}},\ u_{B_{k2}}^{\Delta_q^{S_n^k}}\right) &= \left(l_{k1}^{S_n^k}+1,\ l_{k2}^{S_n^k}\right)\\
\left(u_{C_{k1}}^{\Delta_q^{S_n^k}},\ u_{C_{k2}}^{\Delta_q^{S_n^k}}\right) &= \left(l_{k1}^{S_n^k},\ l_{k2}^{S_n^k}+1\right)\\
\left(u_{D_{k1}}^{\Delta_q^{S_n^k}},\ u_{D_{k2}}^{\Delta_q^{S_n^k}}\right) &= \left(l_{k1}^{S_n^k}+1,\ l_{k2}^{S_n^k}+1\right)
\end{aligned} \tag{16}$$

The following criterias (17) and (18) determine if the reference vector is located in the triangle formed by the tops A_k, B_k and C_k or in that formed by the tops B_k, C_k and D_k.

u_{refk} is in the triangle $A_kB_kC_k$ if:

$$u_{refk\,1}^{S_n^k}+u_{refk\,2}^{S_n^k} < l_{k1}^{S_n^k}+l_{k2}^{S_n^k}+1 \tag{17}$$

u_{refk} is in the triangle $B_kC_kD_k$ if:

$$u_{refk\,1}^{S_n^k}+u_{refk\,2}^{S_n^k} \geq l_{k1}^{S_n^k}+l_{k2}^{S_n^k}+1 \tag{18}$$

C. Calculation of application times

If tops x_k, y_k, z_k corresponding has A_k, B_k, C_k, respectively, the application times are calculated by:

$$\begin{aligned}
t_{y_k}^{\Delta_q^{S_n^k}} &= \left(u_{refk\,1}^{S_n^k}-l_{k1}^{S_n^k}\right)T_s\\
t_{z_k}^{\Delta_q^{S_n^k}} &= \left(u_{refk\,2}^{S_n^k}-l_{k2}^{S_n^k}\right)T_s\\
t_{x_k}^{\Delta_q^{S_n^k}} &= T_s-\left(t_{yk}^{\Delta_q^{S_n^k}}-t_{zk}^{\Delta_q^{S_n^k}}\right)
\end{aligned} \tag{19}$$

Where:

$t_{x_k}^{\Delta_q^{S_n^k}}, t_{y_k}^{\Delta_q^{S_n^k}}, t_{z_k}^{\Delta_q^{S_n^k}}$: are times of application of the vectors $u_{x_k}^{\Delta_q^{S_n^k}}, u_{y_k}^{\Delta_q^{S_n^k}}, u_{z_k}^{\Delta_q^{S_n^k}}$ respectively.

x_k, y_k and z_k : are the tops of A_k, B_k, C_k respectively, $q=1…4$.

D. Examples of chronograms

Figure 4 illustrates the pulses of region ($q=1$ for S_1^k). It is about symmetrical signals that have the same states at the center and at the ends.

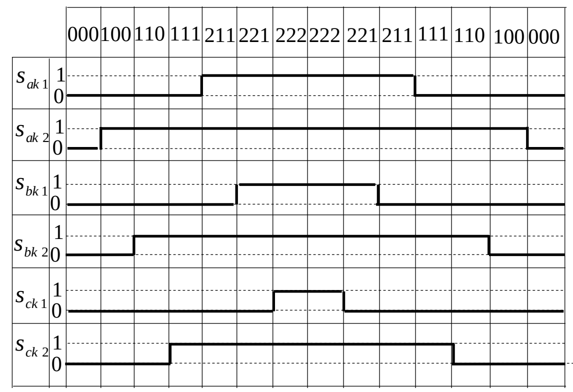

Fig. 4 Examples of chronograms pulses of region ($\Delta_1^{S_1^k}$).

IV. Direct Torque Control

DTC technique is a convenient, relatively complete and easy applicable method. In this method, the required stator flux and torque are determined and a proper switching pattern of the inverter is then applied. Since the motor input voltage contributes in both flux and required torque, a proper switching pattern for inverter firing is essential.

The stator voltage estimator computed using equation (20):

$$\begin{bmatrix}\hat{v}_\alpha\\ \hat{v}_\beta\end{bmatrix} = \left[T\right]\begin{bmatrix}\hat{v}_{s1}\\ \hat{v}_{s2}\end{bmatrix} \tag{20}$$

With: $\hat{v}_{s1}=\left[\hat{v}_{a1}\quad \hat{v}_{b1}\quad \hat{v}_{c1}\right]$, $\hat{v}_{s2}=\left[\hat{v}_{a2}\quad \hat{v}_{b2}\quad \hat{v}_{c2}\right]$

The components of stator flux can be estimated by:

$$\begin{cases}
\hat{\phi}_\alpha(t)=\int_0^t\left(\hat{v}_\alpha-R_s i_\alpha\right)d\tau+\hat{\phi}_\alpha(0)\\
\hat{\phi}_\beta(t)=\int_0^t\left(\hat{v}_\beta-R_s i_\beta\right)d\tau+\hat{\phi}_\beta(0)\\
\left|\hat{\phi}_s\right|=\sqrt{\hat{\phi}_\alpha^2+\hat{\phi}_\beta^2}
\end{cases} \tag{21}$$

The stator flux angle is calculated by:

$$\hat{\theta}_s=\arctan\left(\frac{\hat{\phi}_\alpha}{\hat{\phi}_\beta}\right) \tag{22}$$

Electromagnetic torque calculation uses flux components, current components and pair pole number of the double star synchronous machine [3]:

$$\hat{T}_{em} = p\left(\hat{\phi}_\alpha i_\beta - \hat{\phi}_\beta i_\alpha\right) \tag{23}$$

The reference values of flux and torque are compared to their actual values and the resulting errors are fed into two hysteresis comparators [7].

The switching selection table for the conventional DTC for DSSM is given in tables 3 and 4.

Φ	τ	zone(i)
0	1	$v_{(i+4)L}$
	-1	$v_{(i+8)L}$
1	1	$v_{(i+2)L}$
	-1	$v_{(i+10)L}$

Φ	τ	$zone(i)$ and $zone(i+1)$
0	0	$v_{(i+4)S}$
1	0	v_{iS}

Table 3. First star switching table used in the conventional DTC.

Φ	τ	zone(i)
0	1	$v_{(i+3)L}$
	-1	$v_{(i+7)L}$
1	1	$v_{(i+1)L}$
	-1	$v_{(i+9)L}$

Φ	τ	$zone(i)$ and $zone(i+1)$
0	0	$v_{(i+3)S}$
1	0	$v_{(i+5)S}$

Table 4. Second star switching table used in the conventional DTC.

The general structure of the double star synchronous machine with direct torque control using a three-level inverter in each star is represented by figure 5.

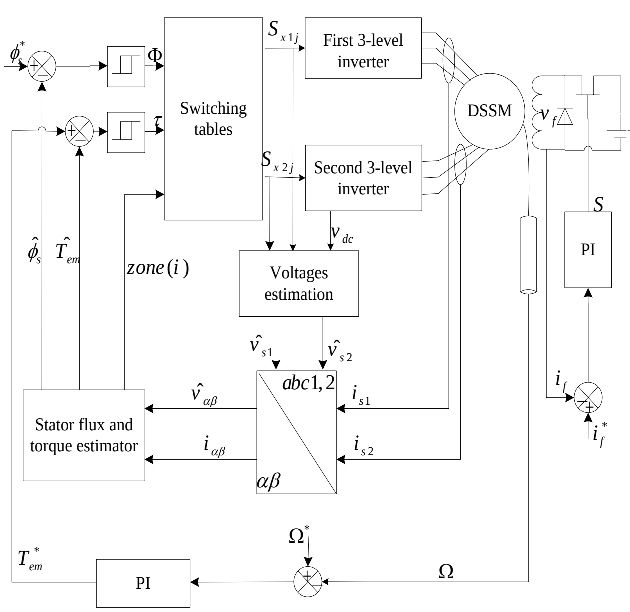

Fig. 5 DTC scheme for DSSM (with *j=1, 2, 3* or *4*).

V. Direct Torque Control Based on Space Vector Modulation

The main idea the DTC-SVM control strategy is to force the torque and stator flux to approach their reference by applying in one sampling period several voltage vectors instead of only one voltage vector as in basic DTC [9]. This control algorithm uses prefixed time intervals within a cycle period and in this way a higher number of voltage space vectors can be synthesized with respect to those used in basic DTC technique.

The presented control strategy is based on simplified stator voltage equations described in stator flux oriented x-y coordinates:

$$\begin{cases} v_x = R_s i_x + \dfrac{d\phi_s}{dt} \\ v_y = R_s i_y + \omega_s \phi_s \end{cases} \tag{24}$$

By applying the following rotation transformation, with transforms variable in the stator flux reference frame *x-y* to the stationary reference α-β :

$$\begin{pmatrix} v^*_{\alpha 1} \\ v^*_{\beta 1} \end{pmatrix} = \left[P(\theta_s)\right]\begin{pmatrix} v^*_x \\ v^*_y \end{pmatrix},\ \begin{pmatrix} v^*_{\alpha 2} \\ v^*_{\beta 2} \end{pmatrix} = \left[P(\theta_s - \gamma)\right]\begin{pmatrix} v^*_x \\ v^*_y \end{pmatrix} \tag{25}$$

With: $\left[P(\theta_s)\right] = \begin{bmatrix} \cos(\theta_s) & -\sin(\theta_s) \\ \sin(\theta_s) & \cos(\theta_s) \end{bmatrix}$

The torque equation is as follows:

$$\hat{T}_{em} = p\left|\hat{\phi}_s\right| i_y \tag{26}$$

Figure 6 represents the DTC-SVM control of DSSM.

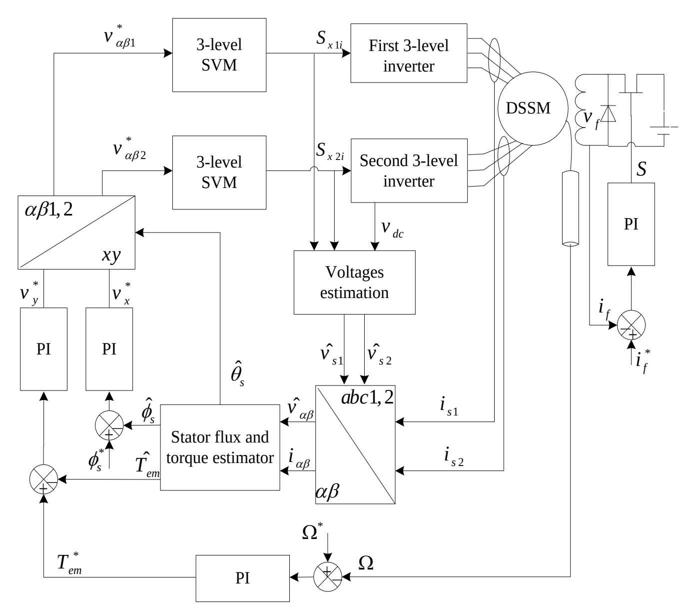

Fig. 6 DTC-SVM of DSSM (with *j=1, 2, 3* or *4*).

VI. SIMULATION RESULTS

To verify the validity of the proposed controller, the system was simulated using the DSSM parameters given in Appendix. The DC side of the inverter is supplied by a constant DC source v_{dc}=*600*V.

The aim of this section is to compare the three-level DTC for DSSM with the three-level DTC-SVM for DSSM. Two situations are considered:

Situation 1: Step change in load torque. The DSSM is accelerating from standstill to reference speed *100* rad/s. The system is started with full load torque (T_L = *11*N.m). After wards, a step variation on the load torque (T_L = *0* N.m) is applied at time t=1.

Situation 2: Step change in reference speed. To test the speed evolution of the system, the DSSM is accelerate from standstill to reference speed (*100* rad/s) afterwards it is decelerate to the inverse rated speed (*-100* rad/s) at time t=*1.5*s.

The dynamic responses of mechanical speed, stator flux and electromagnetic torque are presented in figures 7 and 8 for the conventional three-level DTC and the three-level DTC-SVM respectively. As it can be seen from these figures, the speed response is merged with the reference one and the flux is very similar to the nominal case and independent of the torque.

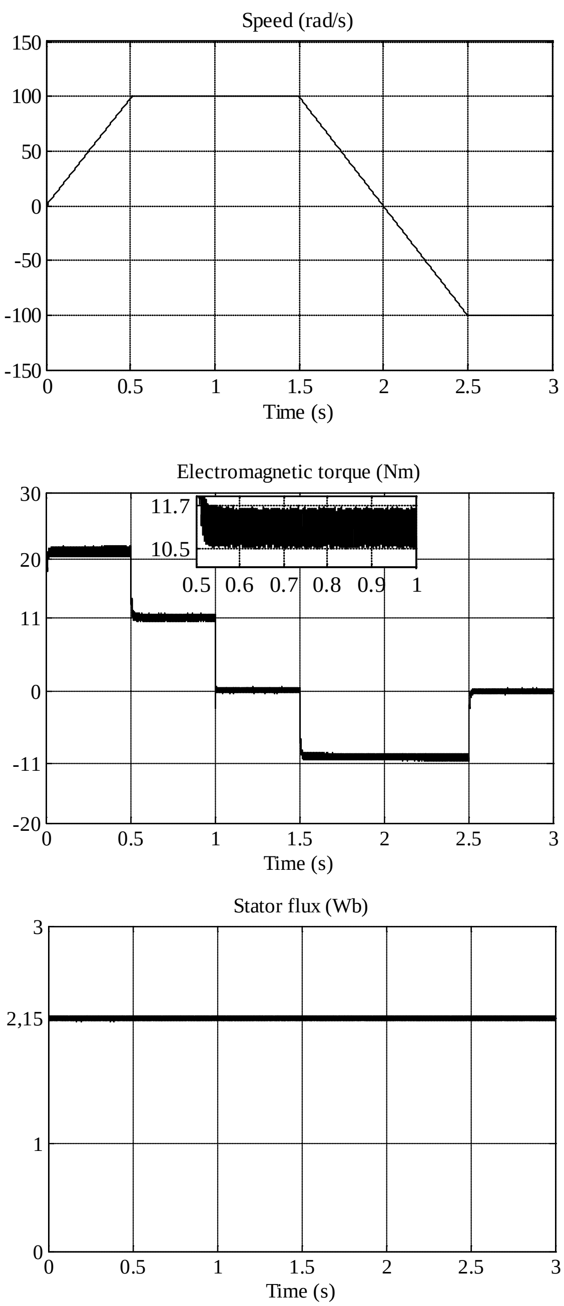

Fig. 7 Dynamic responses of three-level DTC for DSSM.

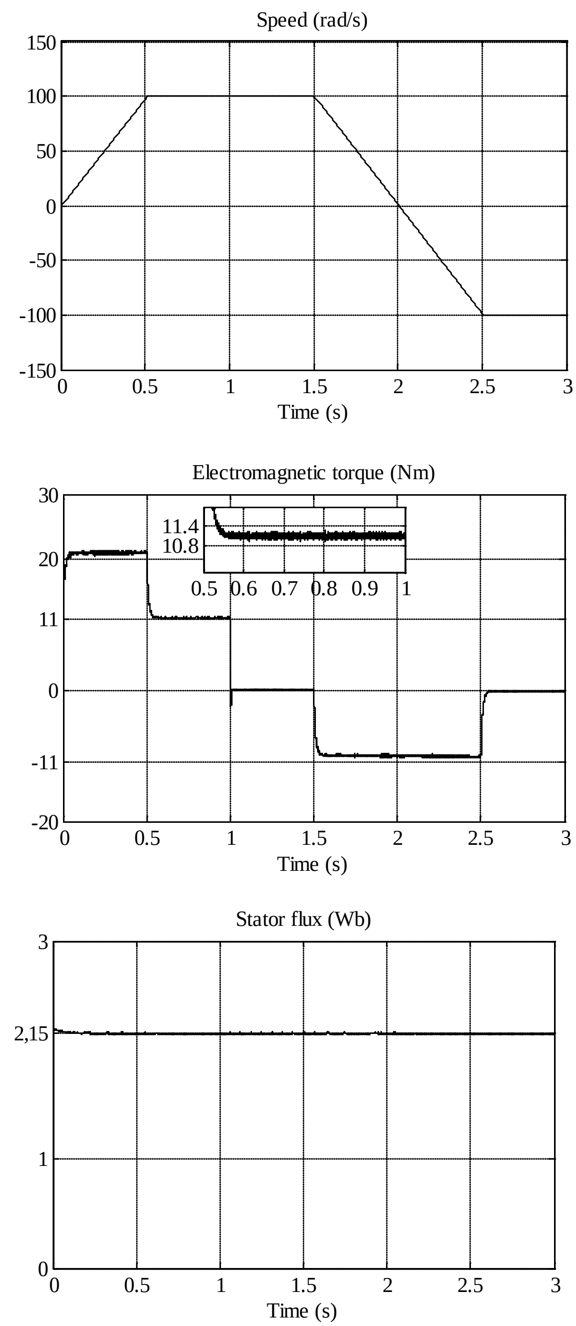

Fig. 8 Dynamic responses of three-level DTC-SVM for DSSM.

Note that the both control approaches ensure good decoupling between stator flux linkage and electromagnetic torque. However the DTC-SVM for DSSM decreases considerably the torque ripple.

Simulations results show that the system controlled by the proposed method is still little affected; it shows a good property of robustness in the face of external load disturbance and speed reversion.

As it can be seen from these figures, the decoupling between torque and flux is ensured in the beginning and during all the control process.

The comparison between figure 7 and figure 8 reveals that the torque ripple and flux ripple of the proposed DTC-SVM are less than that of the conventional one.

VII. Conclusion

The objective of this work was at first, to realize an intelligent control system based on DTC applied to a double star synchronous machine fed by two three-level inverters. In the second place, improving dynamic performance; by introducing the space vector modulation strategy.

In this paper, an effective direct torque control based on space vector modulation strategy of salient-pole DSSM is presented. The direct torque control is a good alternative method for the double star synchronous machine drive system. Indeed, the drive operates with low ripple of motor variables and the decoupling between the stator flux and the torque is maintained, confirms the good performances of the developed drive systems. The simulation results obtained for the DTC-SVM with three-level inverter illustrate a considerable reduction in torque ripple and flux ripple compared to the existing conventional DTC system.

VIII. Appendix

Double star synchronous machine parameters are gathered in Table 5.

5 kW, 2 poles, 232 V, 50 Hz

Components	Rating values
Stator resistance (R_s)	2.35 Ω
Rotor resistance (R_f)	30.3 Ω
Stator inductance d axis (L_d)	0.3811H
Rotor inductance q axis (L_q)	0.211H
Stator inductance (L_f)	15 H
Mutual inductance (M_{fd})	2.146 H
Inertia (J)	0.05Nms2/rad
Friction coefficient (f)	0.001Nms/rad

Table 5. DSSM parameters.

IX. References

[1] L. Emil, "Multiphase Electric Machines for Variable-Speed Applications," IEEE Transactions on Industrial Electronics, Vol. 55, no. 5, December 2009, pp. 1893-1909.

[2] D. Khodja, and C. Boukhemis, "ANN Based Double Stator Asynchronous Machine Diagnosis Taking Torque Change into Account," International Symposium on Power Electronics, Electrical Drives, Automation and Motion, May 2010, pp. 1125-1129.

[3] D. Boudana, L. Nezli, A. Tlemcani, M. Mahmoudi and M. Djemai, "DTC based on Fuzzy Logic Control of a Double Star Synchronous Machine Drive," Nonlinear Dynamics and Systems Theory, Vol. 8, No. 3, 2008, pp. 269–286.

[4] L. Nezli, M. Mahmoudi, M. Boucherit, and M. Djemai, "On Vector Control of Double Star Synchronous Machine with Current fed Inverters," The Mediterranean Journal of Measurement and Control Vol. 1, No. 3, 2005, pp. 118–128.

[5] A. Panda, and Y. Suresh, "Research on Cascade Multilevel Inverter with Single DC Source by Using Three-Phase Transformers," International Journal Electric Power Energy System,Vol. 40, no. 1, 2012, pp. 9-20.

[6] A. Munduate, E. Figueres, and G. Garcera, "Robust Model-Following Control of a Three-Level Neutral Point Clamped Shunt Active Filter in the Medium Voltage Range," International Journal Electric Power Energy System, Vol. 31, no. 10, 2009, pp. 577-588.

[7] V. Talaeizadeh, R. Kianinezhad, S. Seyfossadat, and H. Shayanfar, "Direct Torque Control of Six-phase Induction Motors Using Three-phase Matrix Converter," Energy Conversion and Management, 51(2010), 2482-2491.

[8] S. Kallio, M. Andriollo, A. Tortella, and J. Karttunen, "Decoupled d–q Model of Double-Star Interior-Permanent-Magnet Synchronous Machines," IEEE Transactions on Industrial Electronics, 60(2013), No. 6, 2486-2494.

[9] C. Xianqing, and F. Liping, "New DTC Scheme Based on SVM with Sliding-Mode Observer for Induction Motors," Proceedings of the IEEE International Conference on Automation and Logistics Shenyang, China, (2009), 1484-1488.

E. Benyoussef was born in M'sila (Algeria) in 1985. He received the Eng. Degree in Electrical Engineering from Mohammed Boudiaf University of M'sila in 2009 and the MS degree from the Electrical Engineering Institute of Sidi Bel Abbes University in 2011. He is a member of ICEPS (Intelligent Control Electrical Power System) Laboratory. His research interests are in modeling and robust control of dual three phase synchronous motors and converters.

A. Meroufel was born in Sidi Bel Abbes (Algeria) in 1954. He received his BS degree in electrical engineering from the USTO ran (Algeria) in 1980, the MS degree from the same University (USTO) in 1990 and the PhD degree from the Electrical Engineering Institute of University of Sidi Bel Abbes (Algeria) in 2004. He is currently Professor of electrical engineering in this University. He is a member of ICEPS (Intelligent Control Electrical Power System) Laboratory. His research interests are in robust control of electrical machines, Harmonics analysis methods and improvement of PFC, Non-linear control of electrical drives, Power electronics. He is an author and co-author of more than 30 scientific articles.

S. Barkat received his Engineer, Magister and Doctorate degrees, all in Electrical Engineering, from the Polytechnic National Institute of Algiers in 1994, 1997 and 2008 respectively. In 2000, he joined the Department of Electrical Engineering, University of M’sila. His current research interests are in the field of power electronics, renewable energies, multiphase drives, and advanced control theory and applications.